 SDHM, vol.7, no.3, pp.211-229, 2011

Fatigue Crack Growth in Stiffened Panels, Integrally Machined or Welded (LBW or FSW): the DaToN Project Common Testing Program

A. Lanciotti, L. Lazzeri[1], C. Polese[2], C. Rodopoulos[3], P. Moreira[4,5], A. Brot[6] G. Wang[7], L. Velterop[8], G. Biallas[9] and J. Klement

Abstract: An experimental activity was performed to collect test data on the fatigue crack propagation in various types of specimens, within the DaToN research project, partly funded by the EU in the FP6 programme. Only one general configuration was used, i.e. flat panels with two blade stringers, with different options for the manufacturing processes, that could be integral or welded. The purpose of this test activity was to obtain useful results for the validation and calibration of prediction methodologies, also developed in the same DaToN research project. A wide experimental programme was defined and performed by many laboratories; the materials investigated were 2024-T3 and 6056, welded in the T4 or T6 conditions. The main results are here presented and commented, both for what concerns the fatigue crack propagation tests and the residual stress measurements.

1 Introduction

Many metallic aircraft structures are typically composed by a thin skin, reinforced by riveted stiffeners. The manufacturing of such type of structures is quite expensive, because there are many operations and controls to be performed in preparing a hole and in installing a rivet; just to give an order of magnitude, assembly

[1] Department of Aerospace Engineering, University of Pisa, Italy (Pisa).
[2] Department of Aerospace Engineering, University of Pisa, Italy. (Now with School of Mechanical, Industrial and Aeronautical Engineering, University of Witwatersrand, Johannesburg, South Africa).
[3] Materials Research Institute, Sheffield Hallam University, UK (SHU). (Now with Department of Mechanical Engineering and Aeronautics, University of Patras, Greece).
[4] Institute of Mechanical Engineering, Universidade do Porto, Portugal. (IDMEC).
[5] Israel Aerospace Industries, Israel. (IAI).
[6] Swedish Defense Research Agency, Sweden. (FOI).
[7] Nationaal Lucht- en Ruimtevaartlaboratorium, The Netherlands. (NLR).
[8] German Aerospace Center, Cologne, Germany. (DLR).
[9] Department of Mechanical Engineering, Brno University of Technology, Czech Republic. (Brno).

cost of aircraft structures is about 40 - 50 % of the production cost, [Borradaile (1999)]. As a consequence, alternative design approaches, that use integral and welded structures to replace the conventional built-up structures, are of great interest. Therefore, it is not surprising that aircraft industries dedicate many efforts to a reduction of costs, both trying to introduce automatic riveting as largely as possible and looking for different stringer-to-skin joining techniques. In this respect, various options have reached recently a maturity level that allows them to be considered as serious candidates to replace riveting: in particular High Speed Machining (HSM) is widely applied to obtain integral structures, often of complex geometry, offering significant cost savings due to the strong reduction in part numbers to be fabricated and assembled together. Major shortcomings of HSM are associated with the high waste of material (normally, more than 90% of the initial material is transformed into chips) and, quite often, also in the loss of the advantage associated with the higher resistance in the rolling direction of metallic semi-finished thin products. Interesting alternative manufacturing processes may also be the new welding processes, such as Laser Beam Welding (LBW) and Friction Stir Welding (FSW), which have reached a high level of development, with a strong reduction of the defects normally associated with welding. Discontinuity in metal microstructure (and presence of Heat Affected Zone), residual stresses that often may induce significant geometrical distortion in the component and weld defects are serious problems, that have anyhow been strongly reduced by improvements in the LBW and FSW processes.

The new solutions presented (HSM, LBW and FSW) give rise to an unitary stiffened structure (integral or welded, according to the process), which has a satisfactory behaviour against compression loads, but there are concerns about its durability and damage tolerance characteristics. For this reason, major applications have been focused to aircraft lower fuselage panels, that are normally compressed in flight and for which the fatigue strength requirement plays a minor role. Nevertheless, it is important to understand their damage tolerance behaviour and to develop and validate design methodologies; this was the objective of the DaToN (Innovative Fatigue and Damage Tolerance Methods for the Application of New Structural Concepts) research project, partly funded by the EU within the Sixth Framework Programme and coordinated by IFL (Institut für Flugzeugbau und Leichtbau) of the Tech. Universität Braunschweig. It was considered important to generate a set of experimental data specifically obtained to allow the assessment of prediction methodologies.

2 Test Specimen and Procedure

At the beginning of the program, it was decided to study mainly the crack propagation problem, and in particular the problem of a crack approaching a stiffener. For this purpose, a specimen geometry was defined (Fig. 1), that was basically a plate with two stiffeners: to maintain symmetry the starting defect was introduced in the centre of the panel. The total length of the initial defect, artificially introduced in the panel, was 20 mm. The position of the initial defect is not realistic because there is no stress concentration in that location; anyhow, this situation is critical for the considered specimen and is representative of an actual situation when a long crack approaches a stringer.

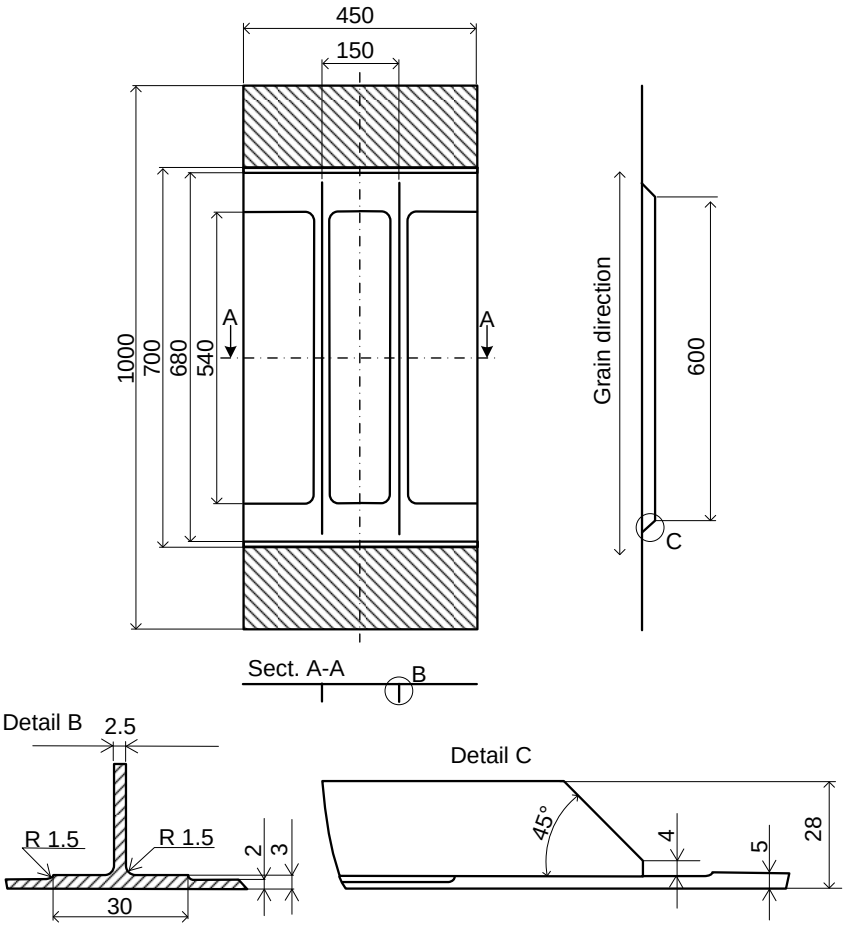

Figure 1: Two stringers specimen geometry. (DATON specimen).

It was decided to investigate crack propagation in panels with the same geometry, but manufactured with different materials and processes; Alcan was interested in the project and provided all the material used to manufacture the specimens. The materials were the traditional 2024 (as a reference material), that was provided in the -T3 or in the -T351 conditions, according to the thickness of the products, and 6056, an alloy developed by Alcan for welded applications, that was provided in the -T4 condition. In this last case, the welded panels were produced in two heat treatments: one option was to treat the -T4 into -T6, then weld and test in the as-welded condition; the other option was to weld in the -T4 condition, then age (four hours at 190 ˚C) to -T6 and then test. Table I summarizes the number and types of specimens that were planned to be manufactured; indeed, some of the welded panels produced were defective and could not be tested.

Table 1: Number and types of specimens planned to be manufactured for the common test program.

Material	LBW1	LBW2	FSW	HSM
6056-T6	10	10	10	15 (-T651)
6056-T4	10	10	10	//
2024-T3	10	10	10	18 (-T351)

Among the partners, both EADS research centres (now Innovation Works) in Ottobrunn and Suresnes were charged with the performance of the welding (LBW in Suresnes, FSW in Ottobrunn), while an external supplier (Horak, in Brno) produced the HSM panels.

Because of the difficulties in the definition and optimization of the process parameters, only a few FSW panels could be produced satisfactorily, but with significant distortion. Other panels were defective because the tool truncated during the welding operations.

For the Laser Beam Welded panels, it was decided to select two different manufacturing processes, with one or two laser beam sources, as shown in Fig. 2; in LBW1 panels two laser beams were used to prepare a corner weld, while in the LBW2 panels the skin was machined in such a way to leave a short foot (1 mm in height) at the beginning of the stringer, so that ideally a butt weld could be made. The two variants have different costs and labour times, obviously.

The test activity was divided among the partners to reduce the time, in such a way that the same test could be repeated in two different laboratories; in such a way, a measure of the scatter and of the reliability of the results was obtained. Test performance guidelines were distributed to the participants, to be followed as strictly

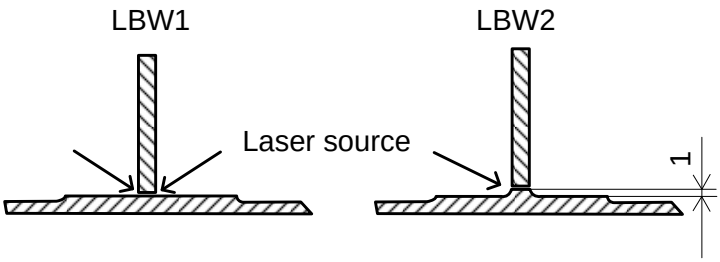

Figure 2: Two different configurations for laser beam welded panels.

as possible, to guarantee that the scatter in the results could be attributed only to the natural scatter in crack growth and not ascribable to systematic differences in the test procedure. Table II shows the partners involved in the testing of the various specimens and the number of tests performed; laboratory acronyms are given in the authors' affiliations in the first page. The originally programmed numbers of tests included in table I were reduced, as a consequence of difficulties and problems in the manufacturing.

The specimen, Fig. 1, is a 2-stringer panel, that was tested with the objective of collecting crack growth data useful to assess the prediction models developed in another Work Package of the project. An artificial crack starter (through crack, 20 mm of total length) was introduced in the centre of the panel, so that during the test the crack tip approaching and passing the stringer could be observed. The test was carried out under Constant Amplitude tension load conditions: two stress ratios (R=0.1 and 0.5) were selected, and different maximum reference stresses were recommended (gross stress 80 MPa for the R=0.1 tests and 110 MPa for the R=0.5 tests, obviously referred to the central section of the specimen) in order to guarantee a relatively quick crack start.

Preliminary non-linear Finite Element analyses of the specimen under maximum load showed that the secondary bending was not of great importance, and in particular was not capable of inducing compressive stresses on the top of the blade stringer; consequently, for the sake of simplicity, no anti-buckling guides were recommended in the crack growth tests. In this way, the specimen faces were completely free, so that crack length measurement, by means of visual methods, was easier. In each participant laboratory a detailed strain gauge survey was carried out on the first specimen, confirming the validity of the FE analyses as well as the uniform gripping and load introduction systems. Moreover, a minimum strain gauge instrumentation was recommended on all the other specimens, in order to

Table 2: Number of specimens actually tested in the different laboratories.

Process	Material	IAI	FOI	Brno	IDMEC	Pisa	SHU	EADS-F	NLR	DLR
High Speed Machined	2024-T351	6	6	6						
	6056-T651				5	5	5			
Laser Beam Welded Panels, LBW1	2024-T3				3	3	3			
	6056-T6 a.w.					3		5		
	6056-T4 PWHT T6				2	5	3			
Laser Beam Welded Panels, LBW2	2024-T3				3	3	3			
	6056-T6 a.w.				2	5	3			
	6056-T4 PWHT T6				2	5				
Friction Stir Welded Panels, FSW	2024-T3					1			4	3
	6056-T6 a.w.							3		
	6056-T4 PWHT T6				2	3				

verify that similar procedures were followed in all the laboratories taking part in the experimental program, in order to avoid additional reasons for scatter.

3 Results

During the crack propagation tests, the four crack tips were optically measured (on the flat and on the stringer sides, left and right), at fixed time intervals, to collect information about differences in the crack tip position, between the flat and the stringer side.

When the crack reached the stringers and started to propagate also along the web of the stringers, optical measurements of the defects were taken also at the inner and outer side of each stringer. For the sake of brevity these data are not given here.

3.1 HSM panels

HSM panels are real integral structures, that do not have a high reputation for damage tolerance characteristics; the crack can easily cut the stringer, that is therefore unable to perform its function to reduce the stress intensity factor and cannot slow down the crack growth rate. The production process is interesting from the economical point of view and leaves the machined surface with a residual stress field slightly different from the one normally present after traditional machining. This situation may have an impact on the durability of the component and some investigation has been performed on this aspect, [Magnusson (2001)], but the effect on crack propagation behaviour has been considered negligible: in the specific Work Package of the DaToN project dedicated to fatigue crack growth prediction methodologies, these were performed using the basic material properties.

A high level of consistency was obtained in the results obtained from both materials, with a relatively small scatter in the a-N plots. Fig. 3 shows a comparison of results from tests carried out at R=0.1 and Smax equal to 80 MPa for both types of materials. The figure has been obtained, like all the other figures where different crack propagation curves are compared, by translating the various curves horizontally, to a common value of the initial half-crack length, equal to 16 mm. As can be observed, the differences between the curves from various laboratories is quite small; another interesting result is the slightly longer crack growth life of the 6056 panels, with respect to the panels made of the high-reputation 2024 alloy.

As far as the crack propagation in the stringers is concerned, in the tests carried out at R=0.1 it has been observed that, even if with some scatter, the crack tip, after having reached the stringer foot, propagates with the same rate in the skin (beyond the stringer) and in the stringer itself, confirming observations reported in [Poe (1971)]. At the higher load used in the tests carried out at R=0.5, instead, the

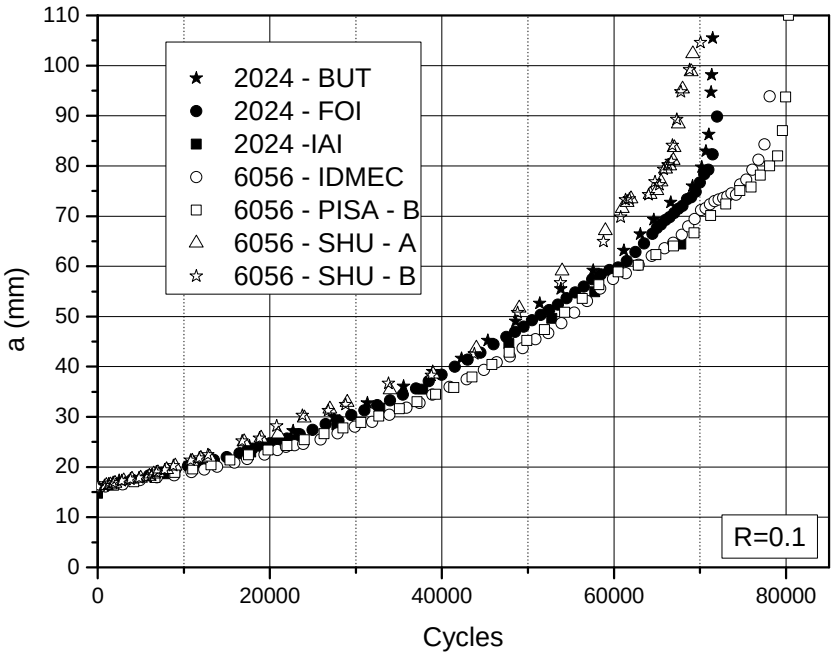

Figure 3: Comparison of data from 2024-T351 and 6056-T651 HSM panels, R=0.1

crack propagates faster in the skin. This behaviour was also shown, with a good approximation, by the welded panels.

3.2 LBW panels

The experimental results have shown small differences between the LBW1 and LBW2 configurations. Fig. 4 shows photographs of the two weld beads, which do not differ significantly from a geometric point of view; due to the small thickness of the sheet available to manufacture LBW2 panels, the foot of the stringer available was only 1 mm in height, that was not sufficient for a complete butt joint, as shown in Fig. 4. The LBW1 configuration was manufactured using two laser sources, while only one was used for LBW2 panels, but this difference does not bring much consequences from the fatigue crack propagation point of view. On the contrary, the weld bead appearance is much different in the two cases, with LBW2 configuration showing a high notch effect at the bead foot; this could be responsible of serious problems for loads applied perpendicular to the stringer direction, but this aspect was not evaluated in the project.

Fig. 5 shows a comparison between the results obtained from 2024 panels tested

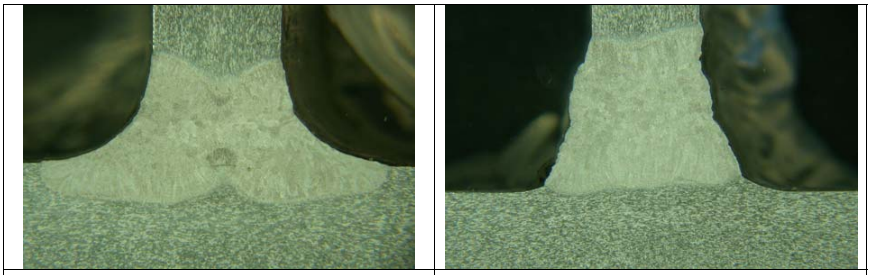

Figure 4: Micrographs of the LBW beads.

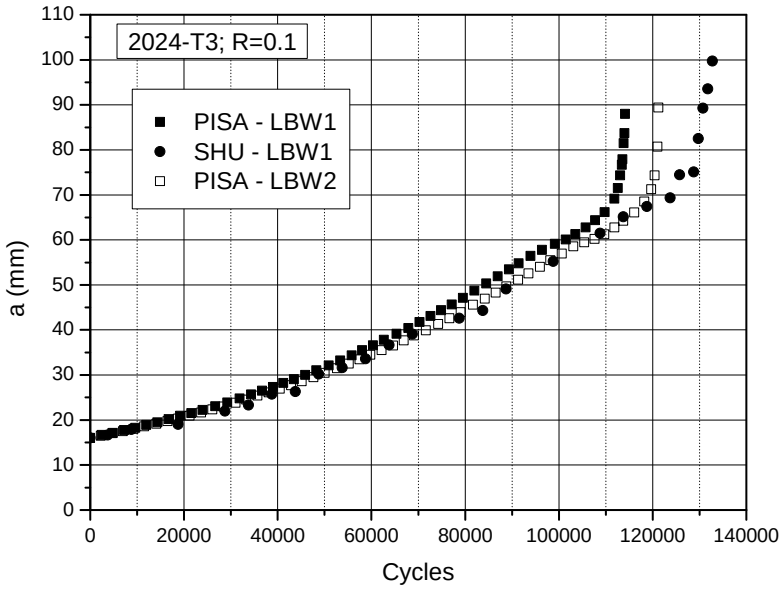

Figure 5: Crack growth curves for the two LBW configurations (2024, R=0.1).

under R=0.1 load conditions. A similar situation occurs also for the R=0.5 stress ratio, with crack growth curves, obtained in the different laboratories, almost overlapped.

The influence of the heat treatment can be assessed in LBW panels in 6056 alloy, where two alternatives are available: in the first one the welding was performed in the T4 condition and afterwards the panel was subjected to ageing (4 hours at 190 $^{\circ}$C); these panels are referred to as Post Weld Heat Treated, PWHT. In the second

alternative, the material was brought to the T6 condition and then welded (and later tested in the as-welded condition). Fig. 6 shows results from LBW2 panels, tested under R=0.1 and Smax = 80 MPa, which quite clearly show that PWHT panels have longer fatigue lives.

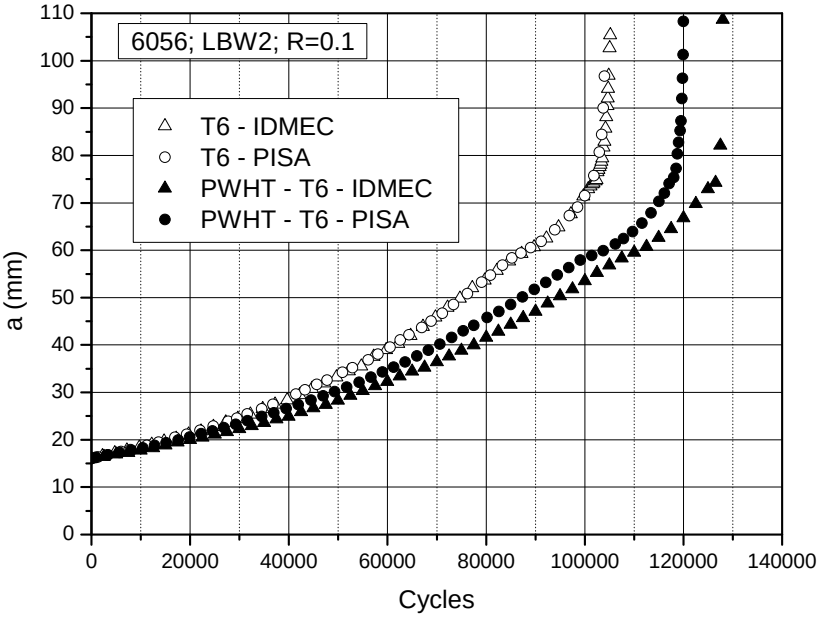

Figure 6: Effect of heat treatment in LBW2 panels. R=0.1.

For the case of R=0.5 loading, the differences between the two conditions are much smaller; the curves, shown in Fig.7, are almost in the same scatter band.

Generally speaking, the results from the tests carried out at R=0.5 have been important for the research, but their significance is lower from the phenomenological point of view: quite often the crack propagation curves of the different configuration are very similar. For this reason these results will not be shown anymore in the following.

From a comparison between Figs. 5 and 6, the behaviour of 2024-T3 results to be equivalent to the one of 6056 panels, welded in the T4 condition and then treated to the T6 condition, while a lower fatigue performance is shown by the 6056 panels welded in the T6 condition and tested as-welded.

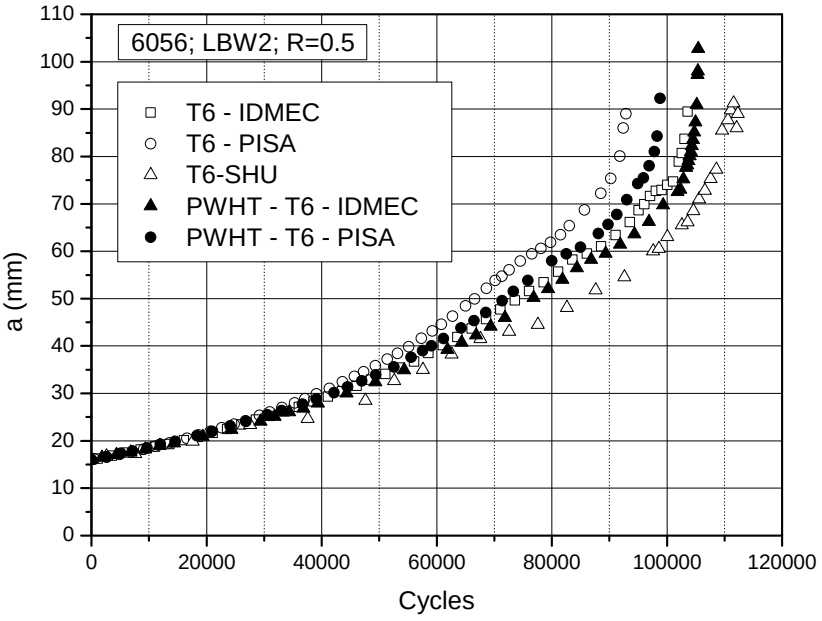

Figure 7: Effect of heat treatment in LBW2 panels. R=0.5.

3.3 FSW panels

Fig. 8 shows the results of the tests performed on the FSW panels. In this case, a higher crack growth rate is observed in the 6056 panels with respect to those in 2024 alloy.

Fig. 9 shows a synthesis of all the results of the crack growth tests. The results are shown by average curves of the various groups of tests. In particular, for the HSM panels, only one curve is reported, due to the low differences for the two materials examined. Similarly, also LBW1 and LBW2 panels results have been merged in one average curve.

It is important to note that it is not possible to speak of a ranking of the various processes. In an integral structure, i.e. not welded, the rate of growth of a defect decreases when the tip approaches a stringer, and increases once that the stringer has been passed. For the geometrical case examined, the failure condition is reached almost immediately after the crack has passed the stringer, so that the decreasing rate in the stringer approach is very evident while, once the crack tip has passed the stringer, the crack growth rate is anyhow very high, since the critical failure condition is approaching very quickly.

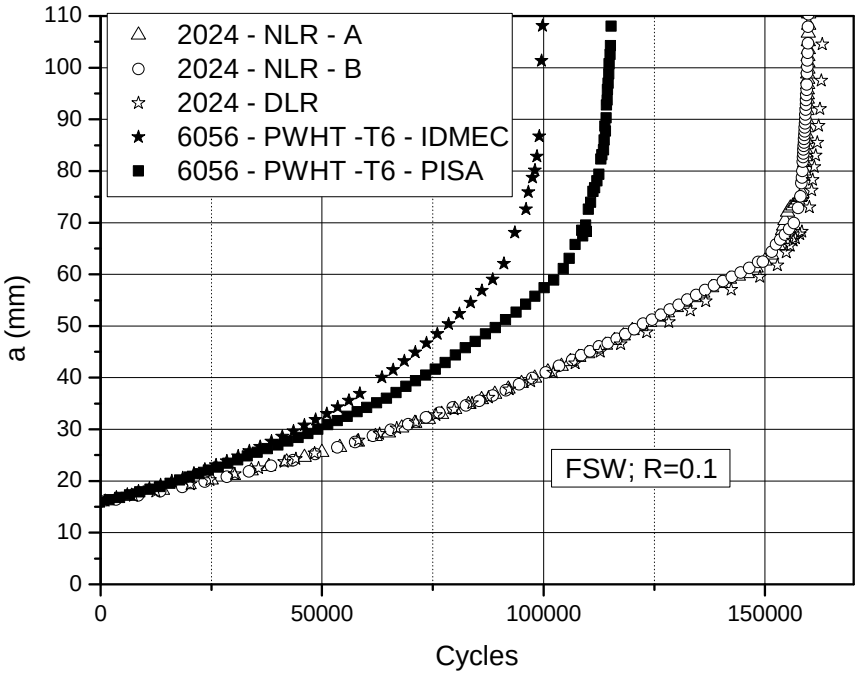

Figure 8: Comparison of crack growth results of FSW panels.

The presence of a welding adds complexity to the problem; in addition to other consequences, a self equilibrated status of residual stresses is produced, which is characterized by tension stresses in the proximity of the weld bead and of compression stresses at a certain distance. The defect, growing towards the welded stringer, firstly propagates in the area where residual compressive stresses are present; the intensity of such residual stresses is higher for higher tensile stress at the weld bead and it has a big retardation effect on the crack growth. It is thus evident that it is improper to speak of "merit" of a process that produces higher residual stresses.

To discuss the results of the propagation tests correctly, it is at this point necessary to describe the activity performed to characterize the residual stress field introduced by the various welding processes.

4 Residual Stresses in Welded Panels

4.1 Measurement of the residual stresses in welded panels

The assessment of the residual stresses in a welded structure is not a trivial problem. Various techniques exist, which differ in methodologies and required instrumenta-

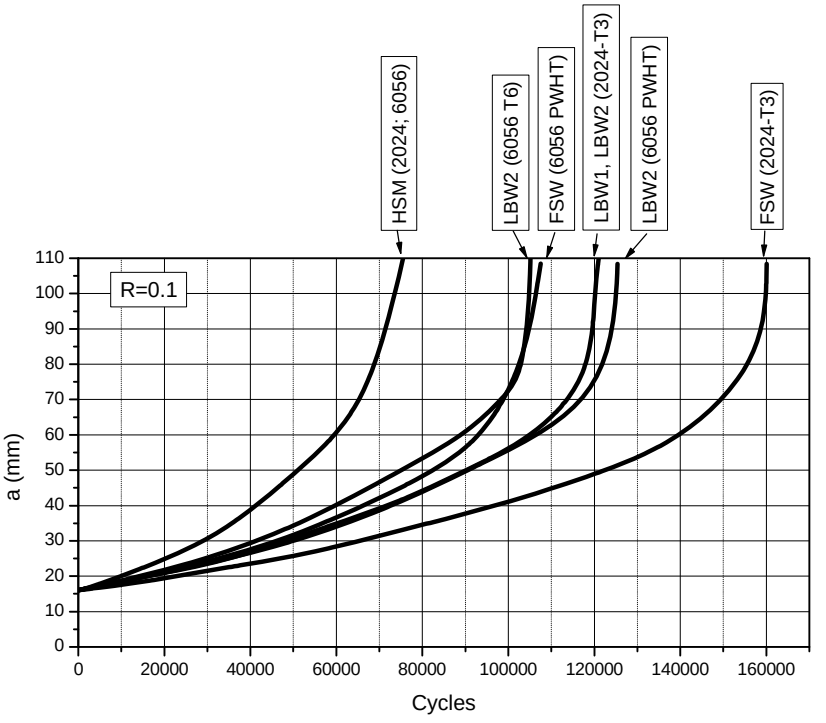

Figure 9: Comparison of mean curves from the various panels tested.

tion.

In the present activity, residual stresses were measured using a destructive sectioning method. For the sake of brevity, only the information required for the application of the method is described in the present paper. A detailed description of the methodology is given in [Ivetic et al (2009)].

Strain gauges are bonded in the area of interest; then, the structure is sectioned to allow the relaxation of the residual stresses. Measuring the difference between the final relaxed state and the initial deformed configuration it is possible to obtain the residual deformation present in the structure.

This technique is conceptually simple and can be performed with cheap equipment, commonly available in material test laboratories. The main disadvantages are the destruction of a coupon and the laborious phase of strain gauge bonding. Each panel analysed was instrumented by 62 strain gauges bonded on the transversal section. Strain gauges were positioned in couples (back-to-back) on both skin panel

sides and on the stringer web too.

Obviously, during the panel sectioning, the strain gauges and their electrical connections must be appropriately protected from possible damages.

In the experimental activity on the DaTon panels, most attention was paid to the evaluation of the residual stress acting in the longitudinal direction, i.e. the stringer direction, the most important from a practical point of view because it superimposes to the stress deriving from the external load.

The residual stresses re-distribute as crack grows. Some measurements, whose results are not given here, were specifically carried out to characterize the redistribution of residual stresses as a function of crack length.

HSM panels were supposed to be free from residual stresses.

4.2 Results of the residual stress measurements

Fig. 10 shows the plot of the longitudinal residual stresses measured in the 2024-T3 panels made by means of the three different production processes: LBW1, LBW2 and FSW. In this figure, as also in the following one relevant to 6056, only the results of the measurements performed on the skin are shown. Also shown are the measurements on the pad, even if this is positioned at a slightly different level with respect to the skin. For simplicity, the results of the measurements made on the stringers are not shown. In each diagram two curves are present, one relevant to the internal (stringer) side and the other one relevant to the external (flat) side.

The three diagrams of the Fig. 10 are very similar to each other, both in the shape and in the peak values. As could be expected, a tension stress is present in the stringer area, with small variations in the thickness direction (i.e. similar values are read on the back-to-back strain gauges). The area interested by tensile stresses is approximately as wide as the pad (30 mm). The peak stress is about 100 MPa. In the other zones of the panel (the central part and the two lateral parts of the panel) compressive stresses are present, with a maximum value of about 40 MPa.

At a first glance, there is equilibrium between the tension loaded and compression loaded areas. This seems a trivial observation, but in some cases experimental measurements do not comply with this obvious requirement.

The compressive residual stress present in the panel central part, where the initial defect was located in the crack propagation tests, justifies the life increase of the welded solutions with respect to the HSM panels, that have been considered unaffected by residual stresses.

The results shown are not in agreement with what can be deduced from Fig. 9, in particular for what concerns the higher crack growth rates in the LBW1 and LBW2 panels in 2024-T3 with respect to the FSW panels. As the residual stresses fields

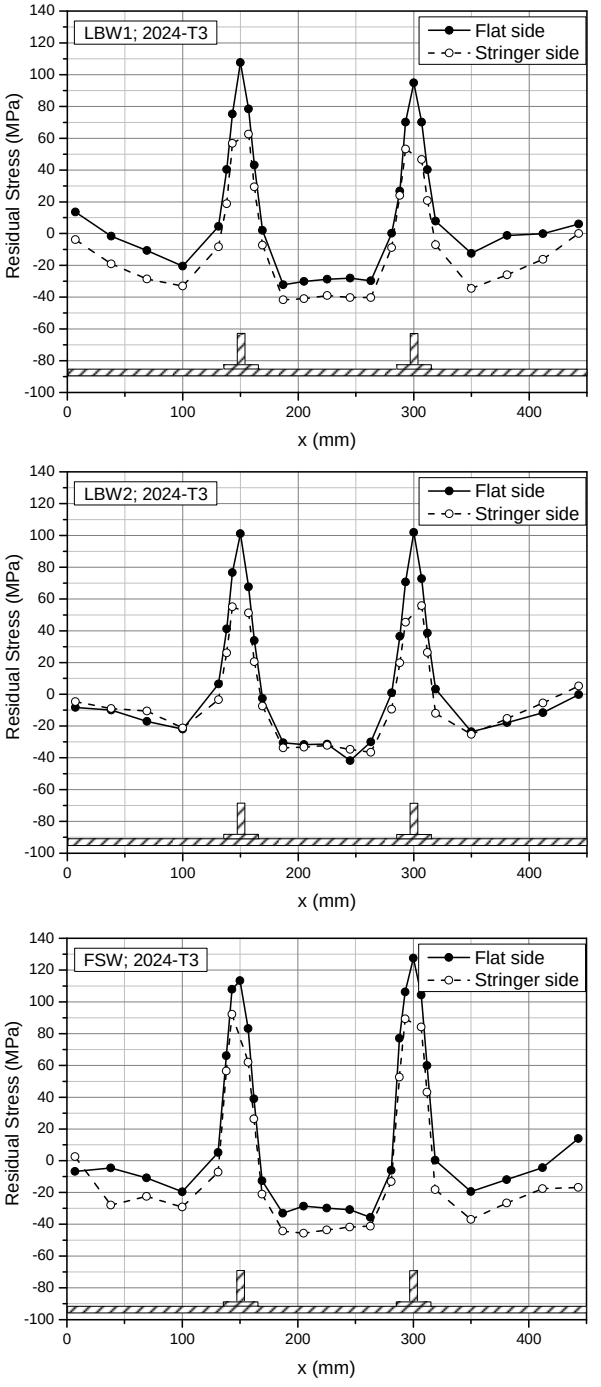

Figure 10: Residual stress measurements in 2024-T3 welded panels.

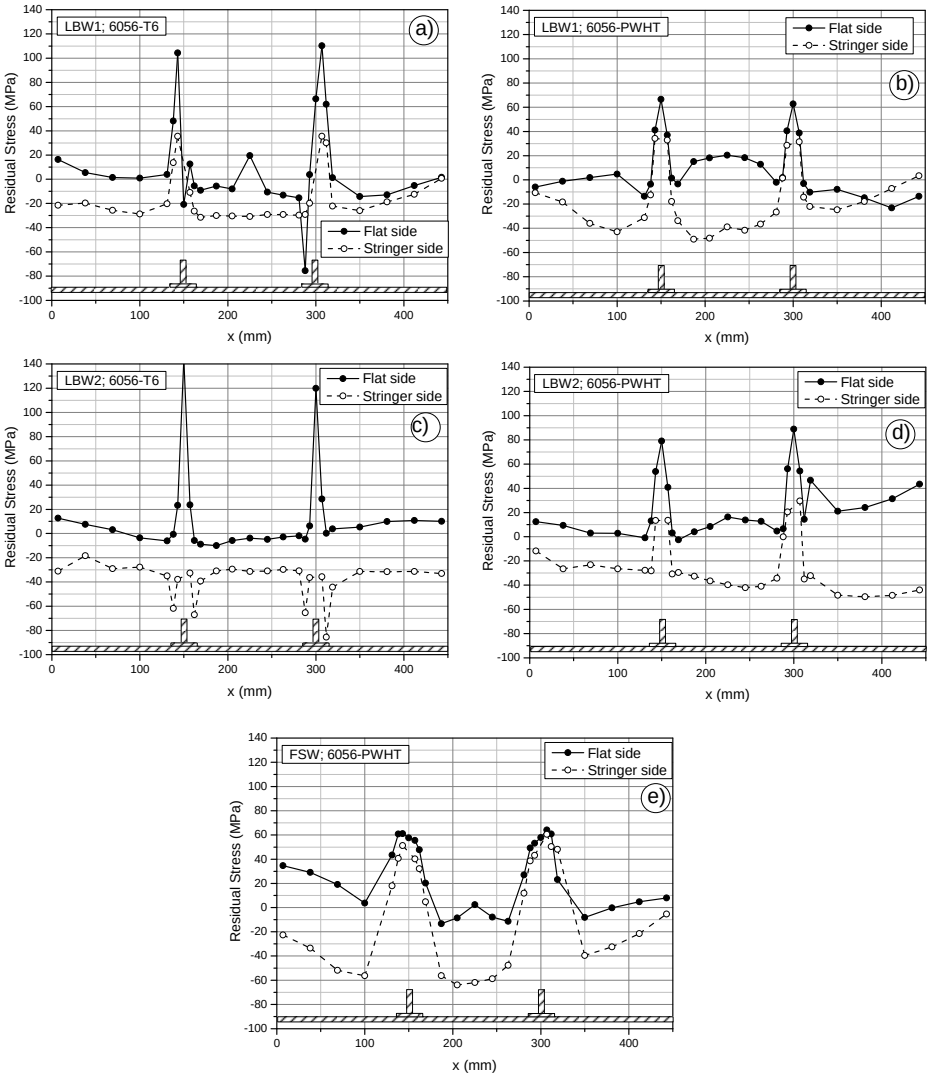

Figure 11: Residual stress measurements in 6056 welded panels.

are comparable, it was logical to expect that also the crack growth rate should be comparable.

Much more complex is the situation for the 6056 panels, for the five different configurations: LBW1 and LBW2, in the -T6 conditions and tested as-welded, or welded in the -T4 heat treatment and then aged to -T6 (Post Weld Heat Treatment)

and the FSW panels, available only in the PWHT condition. Some anomalies show a repeatability that induces to take not clearly identified phenomena into consideration. The two processes LBW1 and LBW2, applied to panels previously treated to -T6, Fig. 11a and 11c, give rise to compressive stresses at the end of the pads in the central bay. In the case of LBW1 these peaks are present on the flat side, in the terminal part of the pads in the central bay. For the LBW2 process, the compression stresses are present on the stringer side, in both terminal parts of the pads. The phenomenon appears to be repetitive and so cannot be put into relation with a defect in the strain gauge measurements. Anyhow, it is not possible to give any plausible explanation of this phenomenon.

With respect to the case of 2024, a higher bending is present (i.e. a larger difference between the stresses measured on the two faces, external/internal). Both tension and compression stresses are comparable with those measured in the 2024-T3 panels, with the exception of the isolated compression peaks, which reach values close to 100 MPa.

The Post Weld Heat Treatment (4 hours at 190 ˚C), necessary to bring the material welded in the -T4 condition to -T6, has the beneficial effect of a reduction of the tension peak, that decreases from 100 MPa to about 60-80 MPa. The compression stress in the centre of the panel remains almost unchanged, while a longer crack propagation life was observed, as shown in Fig. 9. The un-expected compression peaks at the end of the pads disappear, while the difference between the stresses measured on the two sides, i.e. a bending in the central part of the panel, increases; also this phenomenon is repetitive, but not justifiable.

As far as the FSW panels are concerned, a larger extension of the area where a tensile residual stress is present can be observed. This can be, intuitively, attributed to the FSW process that interests a much larger area with respect to the laser process. This phenomenon was not observed in the panels made in 2024-T3.

5 Conclusions

An experimental activity was performed within the DaToN research project, partly funded by the EU within the FP6 programme. The purpose of this test activity was to obtain useful results for the validation and calibration of prediction methodologies, also developed in the same DaToN research project. A reference configuration was identified in the form of flat skin reinforced by two blade stringers. Various production methods were used, such as High Speed Machining, Laser Beam Welding and Friction Stir Welding. Two aluminium alloys were available, 2024 and 6056.

The results from HSM panels were characterized by low scatter; crack propagation rate in 6056 panels was comparable with that of the high reputation 2024-T3.

The LBW panels were available in two configurations which differed in the bead geometry and in the use of one or two laser beam sources. The results demonstrated the substantial equivalence of the two configurations. Moreover, two heat treatment processes were examined in the case of 6056 that was welded in the T4 condition and than aged to T6 or welded directly in the T6 condition.

The behaviour of 2024-T3 was equivalent to the one of 6056 panels, welded in the T4 condition and then treated to the T6 condition, while a lower fatigue performance was shown by the 6056 panels welded in the T6 condition and tested as-welded.

As far as FSW panels are concerned, a higher crack growth rate was observed in the 6056 panels with respect to those in 2024 alloy. Scatter in the results was rather low.

Considering all the results obtained in their globality, it is not possible to speak of a ranking of the various processes, as in the examined configuration the residual stresses, introduced by the welding processes, have a beneficial effect, being most of the propagation life spent in presence of compressive residual stresses.

Residual stresses were characterized, both in terms of peak values and distribution. A destructive sectioning method was used due to its simplicity and efficiency. Strain gauges were bonded in the area of interest; then, the structure was sectioned to allow the relaxation of the residual stresses. Only one panel per type was chosen, assuming that it was representative of all the specimens of the same type.

In the case of specimens made of 2024-T3 similar results were obtained for the different welded panels. A tension stress was present in the stringer area, as expected, with small variations in the thickness direction. The area interested by tensile stresses was approximately as wide as the pad. The peak stress was about 100 MPa. In the other zones of the panel, compression stresses were present, with a maximum value of about 40 MPa.

The compression residual stress present in the panel central part, where the initial defect was located in the crack propagation tests, justified the life increase of the welded solutions with respect to the HSM panel.

The situation for the 6056 panels was much more complex. With respect to the case of 2024, a higher bending was present. Both tension and compression stresses were comparable with those measured in the 2024-T3 panels, with the exception of isolated compression peaks, at the end of the pads; a plausible explanation for these stresses was not found.

The Post Weld Heat Treatment necessary to bring the material welded in the -T4 condition to -T6, reduced the tension peak from 100 MPa to about 60-80 MPa, while the compression stress in the centre of the panel remains almost unchanged;

globally a beneficial effect on the crack propagation was observed.

As far as the FSW panels in 6056 are concerned, a larger extension of the area, where a tensile residual stress is present, was observed. This can be, intuitively, attributed to the FSW process that interests a much larger area with respect to the laser process. This phenomenon was not observed in the panels made in 2024-T3.

References

Borradaile J.B. (1999): Future Aluminium Technologies and their Application to Aircraft Structures, Paper presented at the RTO AVT Workshop onNew Metallic Materials for the Structure of Aging Aircraft, held in Corfu, Greece, RTO MP-25.

Ivetic G., Lanciotti A., Polese C. (2009): Electric Strain Gauge Measurement of Residual Stress in Welded Panels, *The Journal of Strain Analysis for Engineering Design*. Vol. 44, n.1, pp. 117-126.

Magnusson L. (2001): Fatigue of HSM Aluminium Specimens", contribution to the Swedish National Review, 27th Conference of the International Committee on Aeronautical Fatigue (ICAF), Toulouse (FR).

Poe C.C. (1971): Fatigue Crack Propagation in Stiffened Panels. In *Damage Tolerance of Aircraft Structures*, ASTM STP 486, American Society for Testing and Materials, pp. 79-97.